THE JOURNAL OF BIOLOGICAL CHEMISTRY VOL. 285, NO. 27, pp. 20732–20739, July 2, 2010
© 2010 by The American Society for Biochemistry and Molecular Biology, Inc. Printed in the U.S.A.

The Transmembrane Segment of a Tail-anchored Protein Determines Its Degradative Fate through Dislocation from the Endoplasmic Reticulum*

Received for publication, March 5, 2010, and in revised form, April 29, 2010 Published, JBC Papers in Press, April 30, 2010, DOI 10.1074/jbc.M110.120766

Jasper H. L. Claessen, Britta Mueller[1], Eric Spooner, Valerie L. Pivorunas[2], and Hidde L. Ploegh[3]

From the Whitehead Institute for Biomedical Research, Department of Biology, Massachusetts Institute of Technology, Cambridge, Massachusetts 02142

Terminally misfolded proteins that accumulate in the endoplasmic reticulum (ER) are dislocated and targeted for ubiquitin-dependent destruction by the proteasome. UBC6e is a tail-anchored E2 ubiquitin-conjugating enzyme that is part of a dislocation complex nucleated by the ER-resident protein SEL1L. Little is known about the turnover of tail-anchored ER proteins. We constructed a set of UBC6e transmembrane domain replacement mutants and found that the tail anchor of UBC6e is vital for its function, its stability, and its mode of membrane integration, the last step dependent on the ASNA1/TRC40 chaperone. We constructed a tail-anchored UBC6e variant that requires for its removal from the ER membrane not only YOD1 and p97, two cytosolic proteins involved in the extraction of ER transmembrane or luminal proteins, but also UBXD8, AUP1 and members of the Derlin family. Degradation of tail-anchored proteins thus relies on components that are also used in other aspects of protein quality control in the ER.

Terminally misfolded proteins that accumulate in the lumen of the endoplasmic reticulum (ER)[4] are actively transported across the ER membrane into the cytosol. As a consequence of this dislocation (or retrotranslocation), such misfolded products are targeted for proteasomal degradation in a ubiquitin-dependent manner (1).

The ER membrane is the main physical barrier that misfolded proteins must cross and is the arena where dislocation takes place. Different suggestions have been made as to how misfolded products may traverse the ER membrane, ranging from the involvement of lipid droplets or their analogs (2), to a proteinaceous channel (reviewed in (Ref. 3). It is likely that the cell employs different methods of protein extraction, depending on the nature of the folding deficit it diagnoses (4, 5) and the physiological state of the ER during differentiation or while under stress.

One well studied dislocation complex is that exploited by the viral human cytomegalovirus (HCMV) protein US11 (6). US11 is an ER-resident type I transmembrane protein that induces rapid dislocation of newly synthesized Class I major histocompatibility complex (MHC) heavy chains (7, 8). US11 recruits a dislocation complex that minimally consists of Derlin-1/2, the ubiquitin-ligase HRD1, the adaptor protein SEL1L together with the ubiquitin-conjugating enzyme UBC6e, and the auxiliaries AUP1, OS9, and UBXD8 (9–13). The dislocation pathway employed by US11 controls more generally the degradation of aberrantly folded proteins, such as truncated ribophorin (RI_{332}), α_1-antitrypsin null Hong Kong, and the misfolded cystic fibrosis transmembrane conductance regulator ΔF508 (12, 14, 15).

Even though we now know the identity of many components of this dislocation complex, the temporal order and spatial relationship of interactions between these proteins remain elusive. Most of the previously mentioned players in dislocation are anchored in the ER membrane, an important plane of interaction. Misfolded secretory proteins, type I membrane proteins, and polytopic membrane proteins have been the substrates of choice to examine differences and commonalities in their degradative fates, but how the turnover of tail-anchored proteins is controlled remains essentially unknown. We addressed the role of the transmembrane domain (TMD) of UBC6e in its stability and function in an effort to address the behavior of this tail-anchored protein.

The class of tail-anchored (TA) membrane proteins, to which Ubc6e belongs, is a special category of membrane proteins, devoid of a canonical signal sequence to guide their targeting and membrane insertion. Instead, it is the TMD, or tail anchor, located close to the C terminus of the protein, that facilitates post-translational insertion into the target membrane, either independently or through a chaperone system (16). With its TMD so close to its C terminus, it is the principal UBC6e domain available for interaction with other ER proteins. Through TMD replacement, we constructed a set of UBC6e mutants that show the TMD of UBC6e not only to determine its function, but also its stability and mode of membrane insertion. Furthermore, we now describe an extraction pathway for unstable TA proteins and identify not only the deubiquitinating enzyme YOD1 and the ATPase associated with diverse cellular activities

* This work was supported, in whole or in part, by grants from the National Institutes of Health (to H. L. P.). This work was also supported by a fellowship from the Boehringer Ingelheim Fonds (to J. H. L. C.).

[1] Present address: Dept. of Molecular Biology, Simches Research Center, Massachusetts General Hospital, 185 Cambridge St., CP2N7250, Boston, MA 02114.

[2] Present address: Dept. of Molecular and Cellular Biology, Harvard University, Cambridge, MA 02138.

[3] To whom correspondence should be addressed: 9 Cambridge Center, Cambridge, MA 02142. Fax: 617-452-3566; E-mail: ploegh@wi.mit.edu.

[4] The abbreviations used are: ER, endoplasmic reticulum; MHC, major histocompatibility complex; TMD, transmembrane domain; TA, tail-anchored; HC, heavy chains; HA, hemagglutinin; GFP, green fluorescent protein; MS/MS, tandem mass spectrometry; PNGase, peptide *N*-glycanase; WT, wild type.

(AAA) p97 as active players in the removal of a TA protein from the ER membrane, but also UBXD8, Derlins, and AUP1, other components implicated in earlier studies, thus demonstrating convergence with degradation of misfolded ER proteins.

EXPERIMENTAL PROCEDURES

Antibodies, Cell Lines, and Constructs—Antibodies to Class I MHC heavy chains (HC) and UBC6e have been described (11). Antibodies against the hemagglutinin (HA) epitope tag were purchased from Roche (3F10), and anti-FLAG tag was purchased from Sigma-Aldrich. US11-expressing cell lines have been described (12). 293T cells were purchased from American Type Culture Collection. Cell transduced with pLHCX (Clontech)-based vectors were selected and maintained in 125 μg/ml hygromycin B (Roche Applied Science).

The UBC6e, Derlin-1 GFP, Derlin-2 GFP, Derlin-3 GFP, AUP1 GFP, UBXD8 GFP, YOD1, and p97 constructs used for transfection experiments have been described (11, 13, 17). The TMD of UBC6e was replaced by that of CD4 (T4 surface glycoprotein precursor), cytochrome b_5 (type A) or UBC6 by standard PCR-based cloning methods and verified by sequencing (see also Fig. 1).

A cDNA clone for ASNA1 was obtained from Open Biosystems (LIFESEQ1405919) and cloned into pcDNA3.1(+) (Invitrogen) with a C-terminal FLAG epitope tag. Site-directed mutagenesis of ASNA1 G46R and UBC6e-B5 C91S was performed with the QuikChange II Mutagenesis kit according to the manufacturer's instructions (Stratagene).

Transient Transfection, and Viral Transduction—293T cells were transiently transfected using Trans-IT (Takara Mirus Bio) according to the manufacturer's instructions. Virus production in 293T cells and viral transduction have been described (18).

Pulse-Chase Experiments, Immunoprecipitation, and SDS-PAGE—Cells were detached by trypsin treatment and then incubated with methionine- and cysteine-free Dulbecco's modified Eagle's medium with or without the proteasome inhibitor ZL_3VS (50 μM) for 45 min at 37 °C. Cells were labeled with 10 mCi/ml [^{35}S]methionine/cysteine (1175 Ci/mmol; PerkinElmer Life Sciences) at 37 °C for the indicated times and chased with Dulbecco's modified Eagle's medium supplemented with non-radiolabeled methionine (2.5 mM) and cysteine (0.5 mM) at 37 °C for the indicated times. Cells were lysed in 1% SDS. Immunoprecipitations were performed using 30 μl of immobilized rProtein A (IPA 300, Repligen) with the relevant antibodies or with 10 μl anti-FLAG M2-agarose (Sigma) for 3 h at 4 °C with gentle agitation. Immune complexes were eluted by boiling in reducing sample buffer, subjected to SDS-PAGE (10%), and visualized by autoradiography. Densitometric quantification of radioactivity was performed on a PhosphorImager (Fujifilm BAS-2500) using Image Reader BAS-2500 V1.8 software (Fujifilm) and Multi Gauge V2.2 (Fujifilm) software for analysis.

Anti-HA Affinity Purification and MS/MS Analysis—293T cells were transiently transfected with C-terminally HA-tagged UBC6e. The cells were lysed in 2% digitonin, and the lysate was incubated with anti-HA-agarose beads (clone 3F10; Roche Applied Bioscience). Immune complexes were eluted and separated by SDS-PAGE (10%). Polypeptides were revealed by silver staining, excised, and treated with trypsin. Peptides were sequenced by liquid chromatography (11).

Immunoblotting—For immunoblot analysis, cell lysates were prepared by solubilizing cell pellets in 1% SDS. Protein concentrations of the lysates were determined by using the BCA assay (Pierce), and equivalent amounts of total cellular protein were used for immunoblotting.

Fractionation—For subcellular fractionation assays, cells were homogenized by passage through a 23-gauge needle in hypotonic buffer (20 mM HEPES, pH 7.5, 5 mM KCl, 5 mM $MgCl_2$, 1 mM dithiothreitol, supplemented with a protease inhibitor mixture (Roche Applied Science)). The particulate and soluble fractions were separated by centrifugation at 128,000× *g* in a Beckman TLA 100 centrifuge. All samples were adjusted to 0.5% SDS and analyzed by SDS-PAGE (10%).

Peptide N-Glycanase F (PNGase F) and Phosphatase Treatment—PNGase F digestion or phosphatase treatment (10 units) of radiolabeled UBC6e variants was performed after immunoprecipitation according to the recommendations of the manufacturer (New England Biolabs and Fermentas, respectively). Phosphatase inhibitor mixture was acquired from Roche Applied Science and used according to their instructions.

RESULTS

TMD of UBC6e Is Important for Its Role in Dislocation—UBC6e is a tail-anchored membrane protein. To understand the contribution of the TMD of UBC6e to its membrane insertion and stability, we made a set of mutant proteins in which we replaced the TMD of UBC6e with that of CD4 (a type I membrane protein), cytochrome b_5 (a TA protein), UBC6 (a TA protein), as well as a version of UBC6e without its TMD (Fig. 1).

We identified UBC6e as part of a protein complex involved in dislocation of Class I MHC products in cells that express the HCMV immunoevasin US11 (11). Overexpression of UBC6e impairs dislocation of Class I MHC HC by US11. To characterize the mutant versions of UBC6e, we introduced them into U373 astrocytoma cells that stably express US11 and examined dislocation of Class I MHC HC in a pulse-chase experiment. In control cells transduced with the empty pLHCX vector, the labeled HC population is dislocated from the ER to the cytoplasm over the 30-min chase period. We added the proteasome inhibitor ZL_3VS to stabilize the dislocated HC, which accumulates as a diagnostic deglycosylated intermediate due to the action of the cytosolic enzyme PNGase (7, 8). Like the WT enzyme, overexpression of UBC6e-CD4 impaired dislocation of the HC, but none of the other UBC6e mutants produced this effect (Fig. 2). We conclude that the identity of the TMD appended to UBC6e determines its role in dislocation.

TMD of UBC6e Determines Its Stability—Why do some of the newly crafted tail-anchored versions of UBC6e fail to inhibit dislocation? We assessed the stability of the various UBC6e mutants in pulse-chase experiments. Whereas WT UBC6e, ΔTMD and UBC6e-CD4 are stable over a chase period of 3h, both UBC6e-B5 and UBC6e-6 are rapidly degraded (Fig. 3*A*). In fact, no Ubc6e-B5 or UBC6e-6 could be detected at steady-state levels by immunoblotting (Fig. 3*B*). Both unstable mutants are degraded with different but surpris-

ingly rapid kinetics. In U373 cells, UBC6e-B5 is no longer detectable 180 min after its synthesis, and UBC6e-6 is eliminated within 90 min.

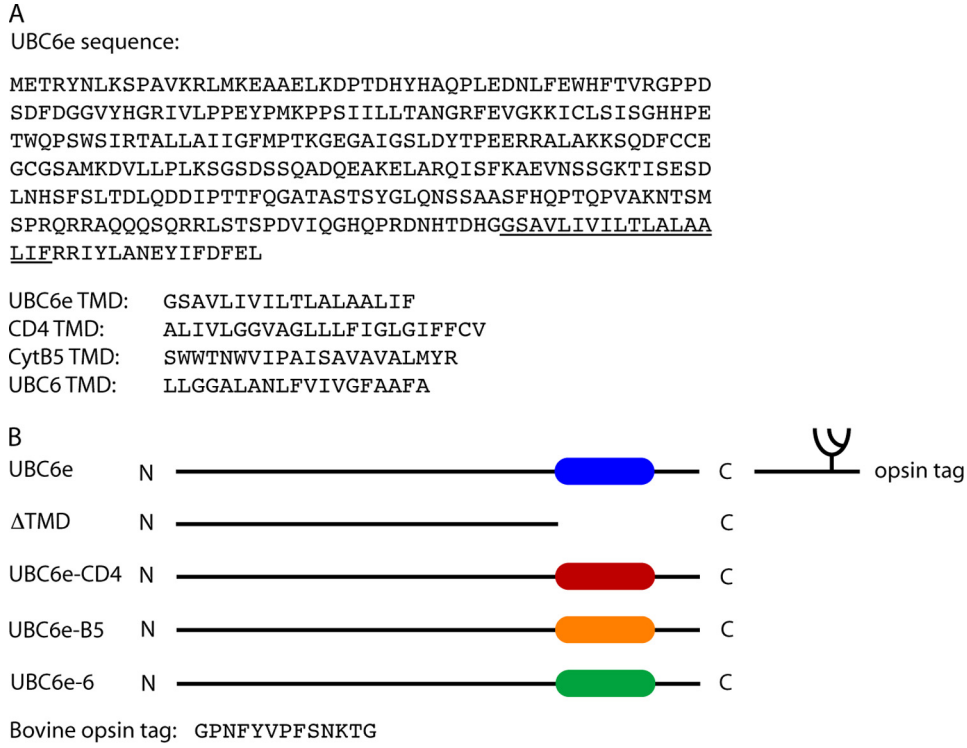

FIGURE 1. **Sequence of UBC6e and the different TMD variants.** *A*, sequence of UBC6e TMD *underlined*. The sequence of the TMD replacements is given and named as indicated. *B*, schematic representation of the different TMD mutants. A 13-amino acid bovine opsin tag was appended to the C terminus of each construct, introducing an *N*-linked glycosylation motif.

The complex banding pattern observed for UBC6e is due to phosphorylation of UBC6e, as shown by treatment with alkaline phosphatase, which eliminates this heterogeneity (Fig. 4) (19).

The short lived UBC6e-B5 and UBC6e-6 mutants were both stabilized in the course of the chase by inclusion of the proteasome inhibitor ZL_3VS (Fig. 3*C*). We conclude that UBC6e-B5 and UBC6–6 are destroyed by proteasomal degradation. This made us wonder whether these unstable UBC6e forms are actually inserted into the ER membrane at all or whether they are immediately targeted for proteasomal degradation upon post-translational release from the ribosome.

All TMD Mutants Are Inserted into the ER Membrane—We explored whether the different versions of UBC6e, regardless of the TMD installed, insert themselves into the ER membrane. To this end, we equipped these variants of UBC6e with a C-terminal bovine opsin tag, a 13-residue sequence that contains an *N*-linked glycosylation motif (Fig. 1) (20). Successful insertion into the ER allows *N*-linked glycosylation of the luminally exposed

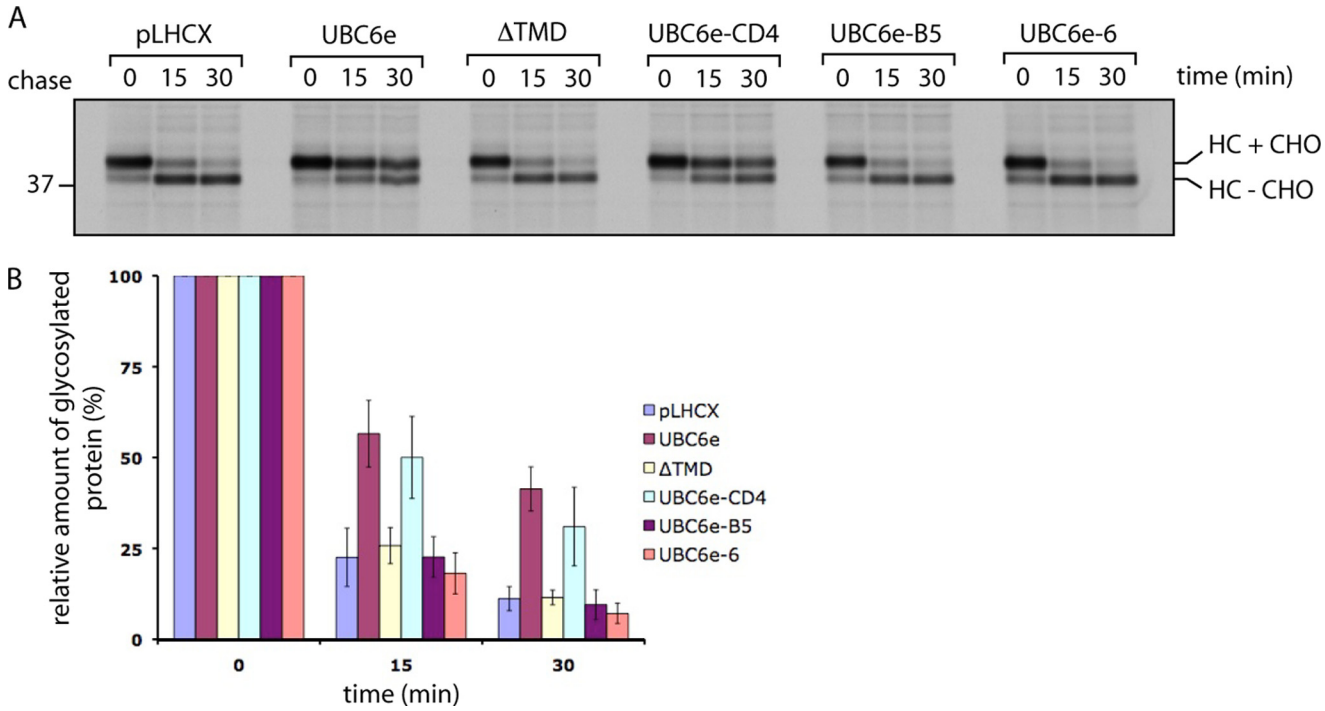

FIGURE 2. **UBC6e and UBC6e-CD4 impair US11-mediated dislocation equally well.** *A*, US11-expressing cells were transduced with either empty vector (pLHCX), UBC6e WT, ΔTMD, UBC6e-CD4, UBC6e-B5, or UBC6e-6. The six cell lines were treated with 50 μM ZL_3VS, pulse-labeled for 10 min with ^{35}S, chased for indicated time points, and lysed in 1% SDS; the lysates were then immunoprecipitated with anti-HC serum. The eluates were separated by 10% SDS-PAGE and visualized by autoradiography. *CHO*, N-linked glycan. *B*, densitometric quantitation of the relative amount of glycosylated HC is shown. *Error bars* represent S.D. ($n = 3$).

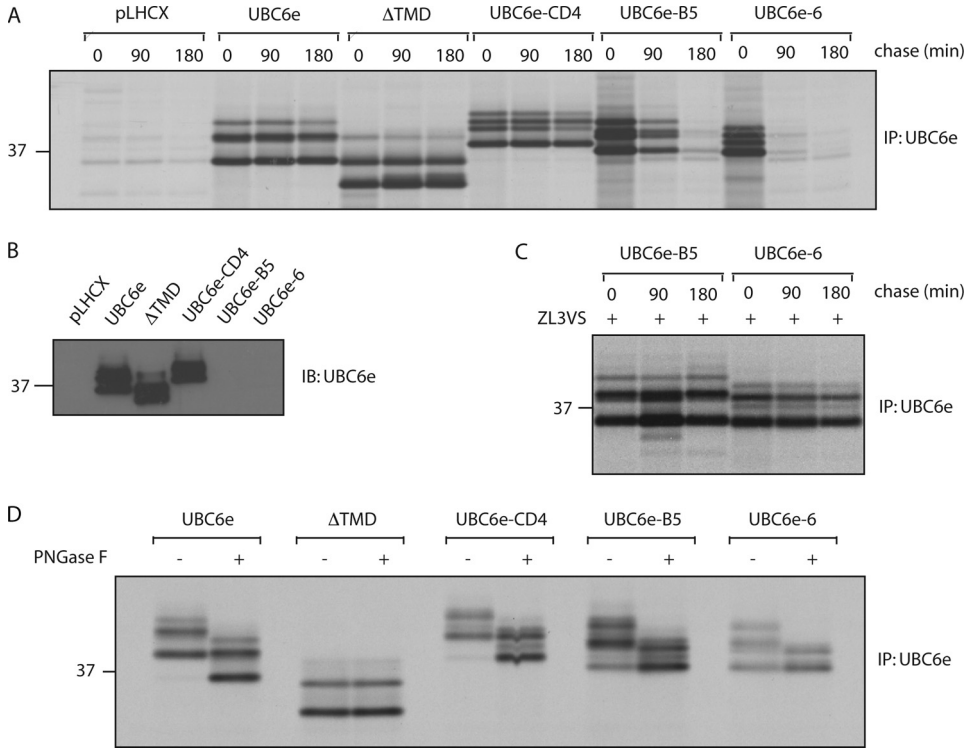

FIGURE 3. **UBC6e and its mutants are inserted into the ER membrane, but only UBC6e-B5 and UBC6e-6 are rapidly degraded.** *A*, the cell lines described in Fig. 2*A* were pulse-labeled for 10 min with ^{35}S, chased for indicated time points, and lysed in 1% SDS; the lysate was then immunoprecipitated (*IP*) with anti-UBC6e serum. The eluates were separated by 10% SDS-PAGE and visualized by autoradiography. *B*, the cell lines described in Fig. 2*A* were lysed in 1% SDS; the lysate was separated by 10% SDS-PAGE and subjected to immunoblotting (*IB*) with anti-UBC6e serum. *C*, the experiment described in *A* was repeated in the presence of 50 μM ZL_3VS. *D*, 293T cells were transiently transfected with the indicated opsin-tagged UBC6e TMD variants. The cells were pulse-labeled for 10 min with 35S, chased for 20 min to allow for membrane insertion, and lysed in 1% SDS. The lysate was immunoprecipitated with anti-UBC6e serum. Where indicated, the eluate was treated with PNGase F for 2 h at 37 °C, separated on 10% SDS-PAGE, and visualized by autoradiography.

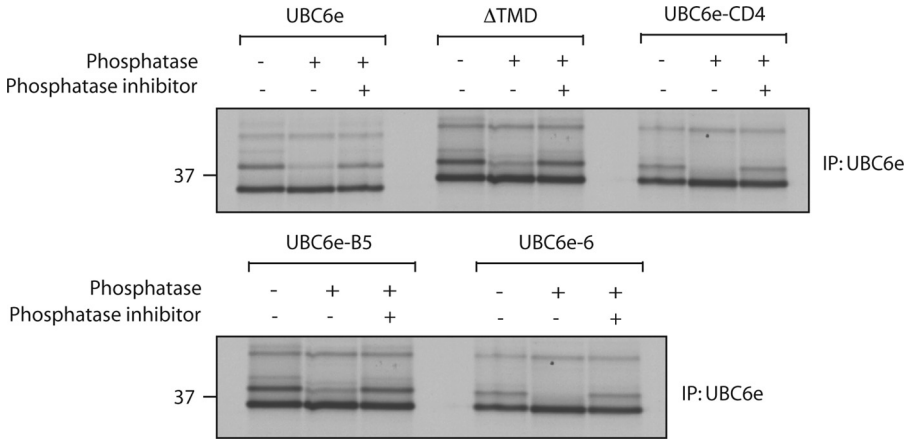

FIGURE 4. **All UBC6e mutants are phosphorylated when expressed in mammalian cells.** 293T cells were transiently transfected with the indicated UBC6e TMD mutants. Twenty-four hours after transfection, the cells were pulse-labeled for 10 min with ^{35}S and chased for 20 min to allow for membrane insertion. The cells were lysed in 1% SDS, and the lysate was immunoprecipitated (*IP*) with anti-UBC6e serum. The immunoprecipitates were treated with alkaline phosphatase (10 units) in the presence or absence of phosphatase inhibitor. The eluate was separated by 10% SDS-PAGE and visualized by autoradiography.

opsin tag to proceed and so reports on the efficiency of the event. The opsin-tagged constructs were transiently transfected into 293T cells, which were then pulse-labeled for 10 min and chased for 20 min to examine membrane insertion, as inferred from the acquisition of an *N*-linked glycan. All but ΔTMD were glycosylated, indicating successful insertion into the ER membrane (Fig. 3*D*). To verify that *N*-linked glycosylation had occurred, we used treatment with PNGase, which produces a size shift if indeed an *N*-linked glycan is present. The slight differences in glycosylation levels between the different UBC6e TMD mutants hint at different insertion efficiency, as measured at the 20-min chase time. We conclude that those forms of UBC6e that have a TMD are inserted into the ER membrane. The short lived tail-anchored versions of UBC6e must be extracted from the ER membrane, but how, and how are they destroyed?

Dislocation of UBC6e-B5 Depends on the ER Dislocation Machinery—Both UBC6e-B5 and UBC6e-6 are novel and unique examples of unstable TA proteins. Because they are targeted to the ER, as inferred from *N*-linked glycosylation, yet are destroyed rapidly, we asked whether any of the known components involved in dislocation plays a role in the turnover of these two species. Many of the proteins involved in substrate recognition and dislocation face the ER lumen and are therefore unlikely to be involved in the active removal of UBC6e-B5 or UBC6e-6. We chose to focus on YOD1, a cytosolic deubiquitinating enzyme required for the removal of misfolded species from the ER (17).

To assess the role of YOD1 in the turnover of UBC6e-B5 or UBC6e-6, we transiently transfected 293T cells with either of the dislocation substrates and co-transfected YOD1 WT or catalytically inactive YOD1, its active site cysteine mutated to a serine. Expression of YOD1 WT did not affect degradation of UBC6e-B5, whereas YOD1 C160S stabilized it (Fig. 5, *A* and *C*). No effect on dislocation was observed in cells transfected with UBC6e-6 (data not shown).

Because YOD1 is a deubiquitinating enzyme, stabilization of UBC6e-B5 by overexpression of YOD1 C160S should lead to the accumulation of polyubiquitinated species. Does the stabilized substrate accumulate as a soluble intermediate regardless of its ubiquitination status, or is it a product that remains associated with the membrane? We transfected 293T cells with UBC6e-B5 together with HA-tagged ubiquitin and either WT or inactive YOD1. We lysed cells mechanically and subjected them to sub-

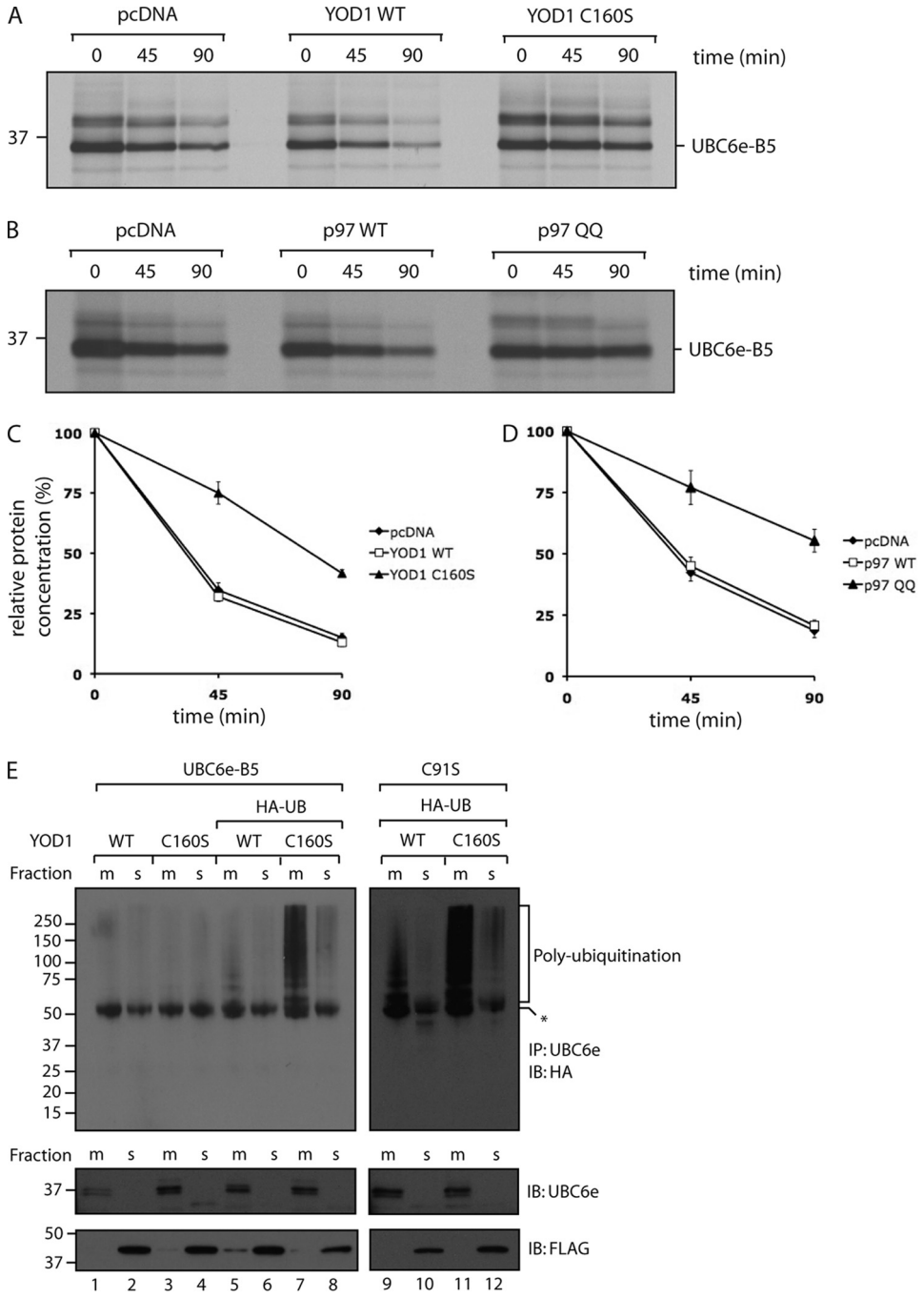

FIGURE 5. **YOD1 and p97 contribute to dislocation of UBC6e-B5.** *A* and *B*, 293T cells were co-transfected with UBC6e-B5 and empty vector, YOD1 WT or YOD1 C160S (*A*). Twenty-four hours after transfection, the cells were pulse-labeled for 10 min with ^{35}S, chased for indicated time points, and lysed in 1% SDS; the lysate was then immunoprecipitated with anti-UBC6e serum. The eluates were separated by 10% SDS-PAGE and visualized by autoradiography. This was repeated for p97 WT and p97QQ (*B*). *C* and *D*, densitometric quantitation of the relative amount of UBC6e-B5 in the presence of YOD1 variants (*C*) or p97 variants (*D*). *Error bars* represent S.D. ($n = 3$). *E*, 293T cells were co-transfected with HA-ubiquitin, UBC6e-B5 WT or C91S and either YOD1 WT or YOD1 C160S. The cells were lysed mechanically in a hypotonic buffer. The membrane and soluble fractions were separated by high speed centrifugation. The individual fractions were lysed in 0.5% SDS and immunoprecipitated (*IP*) with anti-UBC6e serum. Ubiquitinated UBC6e-B5 was visualized with anti-HA antibody. Correct separation of the membrane and soluble fractions was assessed by immunoblotting (*IB*) with anti-UBC6e (membrane fraction) and anti-FLAG for YOD1 (soluble fraction). The *asterisk* indicates nonspecifically detected polypeptides.

cellular fractionation to separate the particulate from the soluble fraction. We performed immunoprecipitation with anti-UBC6e serum on each of the fractions in the presence of detergent and visualized the ubiquitinated species by immunoblotting with an HA-antibody. As expected, co-expression of UBC6e-B5 and YOD1 C160S caused accumulation of polyubiquitinated UBC6e-B5 species predominantly in the membrane fraction (Fig. 5*E*). Correct separation of the fractions was ensured by immunoblotting for UBC6e and YOD1, respectively (Fig. 5*E*). The presence of inactive YOD1 thus stalls dislocation of UBC6e-B5 at the ER membrane.

UBC6e is an E2 enzyme with a catalytic cysteine residue at position 91. To exclude the possibility that the observed polyubiquitin chain is built on the active site cysteine of UBC6e, we repeated the experiment with a form of UBC6e-B5 in which the active site cysteine was mutated to a serine (Fig. 5*E*, *right panel*). No differences in ubiquitination patterns were observed, showing that UBC6e-B5 indeed accumulates as a polyubiquitinated degradation intermediate when co-expressed with YOD1 C160S.

The AAA ATPase p97 helps remove misfolded substrates from the ER (21, 22). As YOD1 interacts with p97 through its UBX domain (17), we also tested the involvement of p97 in the degradation of UBC6e-B5. 293T cells were co-transfected with UBC6e-B5 and either p97 WT or inactive p97 QQ (21). As expected, co-expression with inactive p97 impaired the degradation of UBC6e-B5, implicating p97 in the dislocation of a TA protein (Fig. 5, *B* and *D*). We performed additional experiments that involved the use of dominant negative versions of Derlin-1, -2, and -3, expressed as GFP fusion proteins (13), as well as UBXD8-GFP and AUP1-GFP, all of which have previously been implicated in the removal of misfolded proteins from the ER (9–11, 14). With the exception of Derlin-2 GFP, all of these constructs impaired degradation of Ubc6e-B5 (Fig. 6). Degradation of UBC6e-B5 thus involves at least part of the dislocation machinery involved in protein quality control in the ER.

ASNA1 Targets UBC6e to the ER Membrane—Tail-anchored membrane proteins are characterized by post-translational membrane insertion, which occurs either in a manner assisted

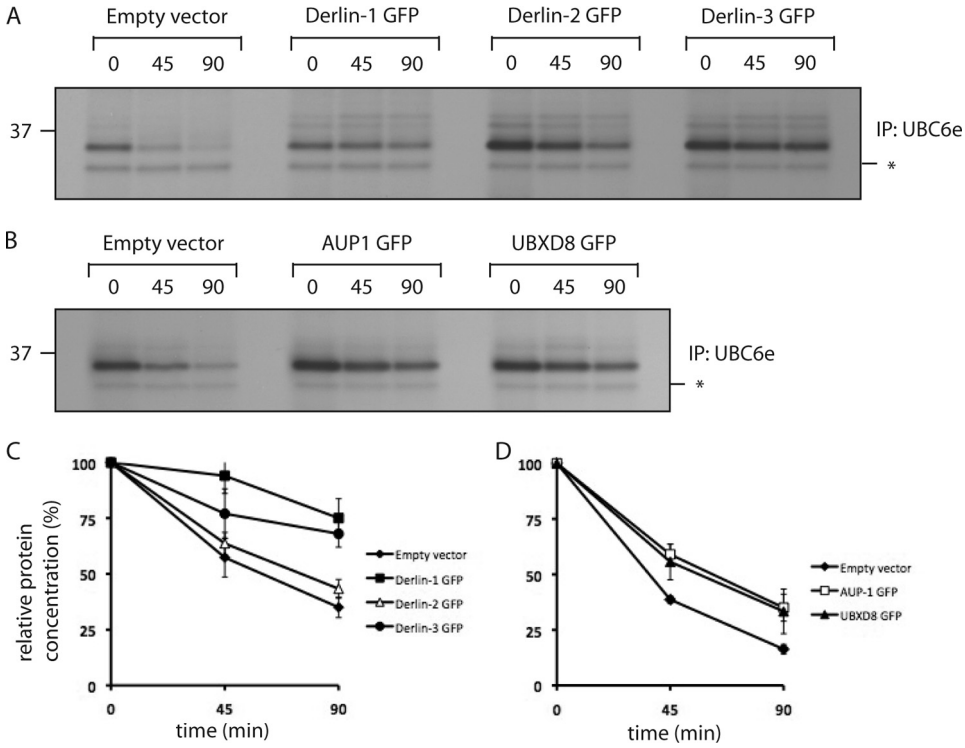

FIGURE 6. **Dislocation of UBC6e-B5 depends on Derlin-1, Derlin-3, UBXD8, and AUP1.** *A*, 293T cells were transiently co-transfected with UBC6e-B5 and either an empty vector control, Derlin-1 GFP, Derlin-2 GFP, or Derlin-3 GFP. The experiment was performed as in Fig. 5*A*. The *asterisks* indicate nonspecifically bound polypeptides. *IP*, immunoprecipitate. *B*, 293T cells were transiently co-transfected with UBC6e-B5 and either an empty vector control, AUP1 GFP, or UBXD8 GFP. The experiment was performed as in Fig. 5*A*. *C* and *D*, densitometric quantitation of the relative amount of UBC6e-B5 in the presence of Derlin family variants (*C*) or AUP1 GFP and UBXD8 GFP (*D*) is shown. *Error bars* represent S.D. ($n = 3$).

by, or independent of, a chaperone system, the composition and function of which are only now being unraveled. In mammalian cells, the client tail-anchored protein can be inserted through ASNA1 (TRC40), heat shock protein 40/heat shock cognate 70, signal recognition particle, or independent of chaperone assistance, depending on the hydrophobicity of the transmembrane segment (16). We identified ASNA1 by MS/MS (47% sequence coverage, 10 unique peptides) as an interaction partner of UBC6e in a large scale immunopurification. In this experiment, C-terminally HA-tagged UBC6e was transduced into 293T cells. UBC6e was isolated by immunoprecipitation from digitonin extracts and the eluate subjected to SDS/PAGE, followed by MS/MS analysis of the individual polypeptides recovered in a complex with Ubc6e. Having recovered ASNA1 as a strong hit, we therefore set out to examine whether membrane insertion of UBC6e is in fact dependent on ASNA1.

ASNA1 is an ATPase involved in posttranslational targeting of membrane proteins (20, 23). The crystal structure of Get3, the yeast homolog of ASNA1, provides insight into the binding of a tail-anchored substrate and its regulated release under the control of ATP hydrolysis (24, 25). Accordingly, we made an ATPase-deficient G46R mutant of ASNA1.

To test whether UBC6e is dependent on ASNA1 for membrane targeting and insertion, we examined membrane insertion in the presence of either ASNA1 WT or ASNA1 G46R, using *N*-linked glycosylation as a readout for insertion of the opsin-tagged TA UBC6e variants into the ER membrane. A short pulse of 5 min allowed us to follow the fate of the newly synthesized population of UBC6e. Within 30 min of chase, virtually all of the newly synthesized UBC6e was inserted into the ER membrane in control cells (Fig. 7). Expression of ASNA1 WT did not impair ER membrane integration. However, expression of ASNA1 G46R reduced membrane integration of UBC6e. We performed a similar experiment with UBC6e-CD4 and UBC6e-B5. Again, UBC6e-CD4 behaved as UBC6e WT and required ASNA1 for membrane integration. In contrast, expression of ASNA1 G46R did not affect insertion of UBC6e-B5 (Fig. 7). We conclude that UBC6e is a TA protein targeted to the ER membrane by ASNA1.

DISCUSSION

The TMD of UBC6e determines its function and its stability. We crafted different mutants of UBC6e in which we replaced its TMD with that of other membrane proteins, including TA and type I membrane proteins. A comparison of different TMD mutants of UBC6e showed that the identity of the TMD determines its role in US11-mediated dislocation of MHC Class I HC products and markedly affects the stability of that version of UBC6e itself.

Expression of either active or inactive UBC6e disturbs the function of the dislocation complex nucleated by SEL1L, presumably by disrupting the proper stoichiometry of the multiprotein complex that serves as (part of) the dislocon (11). Our data show that the TMD of UBC6e is crucial for this property. Deprived of its TMD, UBC6e is no longer targeted to the ER and therefore fails to engage other components of the complex. This is in line with our hypothesis that UBC6e engages its interaction partners within the ER membrane (11). When we substituted the TMD of UBC6e with that of other transmembrane proteins, the nature of the replacement TMD affected both function and stability of the resultant product. Irrespective of the nature of the TMD, all forms of UBC6e were inserted successfully into the ER membrane. It is unclear whether UBC6e interacts directly with other members of the HRD1-SEL1L dislocation complex or whether it does so via an as yet unidentified scaffold protein, as proposed for the yeast Hrd1/Hrd3-ubiquitin ligase (26). The nature of the TMD could affect either one of these interactions. The physicochemical properties of the TMD may also affect location and trafficking of its bearer within the plane of the membrane (27).

A UBC6e mutant with the TMD of CD4 mimics the WT enzyme in both function and stability. WT UBC6e and UBC6e-CD4 are TA proteins targeted to the ER by ASNA1.

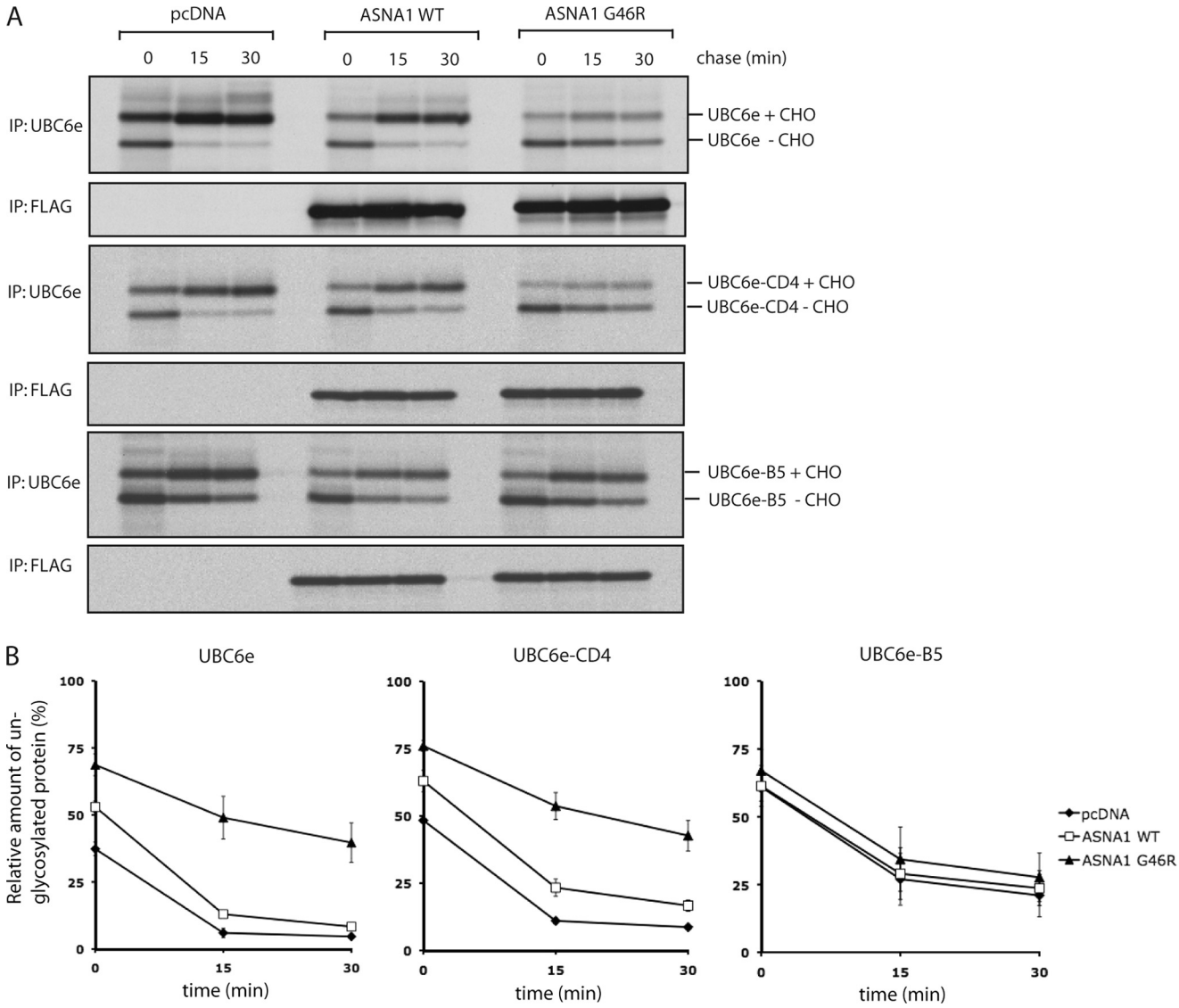

FIGURE 7. **UBC6e and UBC6e-CD4 are targeted to the ER membrane by ASNA1.** *A*, 293T cells were co-transfected with the indicated opsin-tagged UBC6e TMD variants and empty vector, ASNA1 WT, or ASNA1 G46R. Twenty-four hours after transfection, the cells were pulse-labeled for 5 min with ^{35}S, chased for indicated time points, and lysed in 1% SDS; the lysate was then immunoprecipitated (*IP*) with anti-UBC6e serum. The precipitated protein was treated for 1 h with alkaline phosphatase at 37 °C to reduce the complexity of the banding pattern. The eluates were separated by 10% SDS-PAGE and visualized by autoradiography. ASNA1 expression was assessed through immunoprecipitation with anti-FLAG antibody. *B*, densitometric quantitation of the amount of nonglycosylated UBC6e variant relative to total protein is shown. *Error bars* represent S.D. ($n = 3$).

Replacement of the TMD of UBC6e with that of CytB5 or UBC6 results in highly unstable proteins that fail to engage the dislocation complex, as inferred from their inability to affect US11-dependent dislocation of Class I MHC products. After insertion, UBC6e-B5 and UBC6e-6 are rapidly removed from the ER and targeted for proteasomal degradation. Furthermore, UBC6e-B5 does not utilize the ASNA1-dependent pathway for membrane insertion. This unique trait allowed us to use these proteins as substrates to study quality control and active removal of TA proteins.

Both YOD1 and p97 are required for the dislocation of UBC6e-B5 (Fig. 5). In addition, we implicate Derlin-1 and Derlin-3, as well as UBXD8 and AUP1 (Fig. 6), all of which contribute to dislocation (11, 13, 14), in the rapid turnover of UBC6e-B5. This places several known players involved in ER dislocation in a pathway for TA protein degradation (17, 21). The involvement of YOD1, p97, and other proteins that participate in dislocation suggests that the degradation pathway of TA proteins converges with the currently known mechanisms of disposal of misfolded proteins from the ER lumen: ubiquitination triggers active removal of the substrate, which is then targeted to the proteasome. The observed convergence of quality control pathways for ER luminal proteins and for TA proteins must occur downstream of the initial decision to remove the protein from the membrane compartment. The nature of TA proteins places their functional domain on the cytosolic side of the ER membrane. We hypothesize that the initial triage of inserted TA proteins must occur through the action of proteins with a similar cytosolic orientation compared with the ER membrane, or within the plane of the ER itself. The latter possibility would be entirely consistent with the involvement of the Derlins and AUP1 in particular. It is

difficult to envision involvement of the typical ER-resident luminal chaperones such as PDI, OS9, BiP, calreticulin, calnexin, and possibly others.

Both UBC6e-B5 and UBC6e-6 are degraded with rapid but different kinetics. It is unclear why these proteins are dysfunctional and removed, unlike their UBC6e-CD4 counterpart. One possibility is that these TMDs no longer allow interactions with other components of the dislocation complex, triggering an as yet unidentified intramembrane quality control mechanism. Another possibility is that these proteins are mistargeted to the wrong ER membrane subdomains as they no longer engage ASNA1, which targets the tail-anchored UBC6e to the ER membrane, presumably the location where specific receptors for ASNA1 are present. The notion that specific subdomains of the ER may be relegated to quality control and turnover of misfolded proteins is supported by data on the degradation of mutant forms of the polytopic protein Ste6 in yeast (28). By strict analogy with the GET system in yeast (29), membrane receptors could facilitate not only the specific targeting of TA proteins to organelles, but also to unique membrane domains within those organelles. Mistargeting would then result in active removal of the protein. The involvement of YOD1 and p97 in the removal of UBC6e-B5 but not UBC6e-6 may account for the different kinetics for removal and degradation.

Acknowledgments—We thank C. Schlieker, R. Ernst, and J. Damon for helpful scientific discussions.

REFERENCES

1. Ellgaard, L., and Helenius, A. (2003) *Nat. Rev. Mol. Cell Biol.* **4,** 181–191
2. Ploegh, H. L. (2007) *Nature* **448,** 435–438
3. Hebert, D. N., Bernasconi, R., and Molinari, M. (2010) *Semin. Cell. Dev. Biol.*, in press
4. Carvalho, P., Goder, V., and Rapoport, T. A. (2006) *Cell* **126,** 361–373
5. Vashist, S., and Ng, D. T. (2004) *J. Cell Biol.* **165,** 41–52
6. Ahn, K., Angulo, A., Ghazal, P., Peterson, P. A., Yang, Y., and Früh, K. (1996) *Proc. Natl. Acad. Sci. U.S.A.* **93,** 10990–10995
7. Wiertz, E. J., Jones, T. R., Sun, L., Bogyo, M., Geuze, H. J., and Ploegh, H. L. (1996) *Cell* **84,** 769–779
8. Wiertz, E. J., Tortorella, D., Bogyo, M., Yu, J., Mothes, W., Jones, T. R., Rapoport, T. A., and Ploegh, H. L. (1996) *Nature* **384,** 432–438
9. Lilley, B. N., and Ploegh, H. L. (2004) *Nature* **429,** 834–840
10. Ye, Y., Shibata, Y., Yun, C., Ron, D., and Rapoport, T. A. (2004) *Nature* **429,** 841–847
11. Mueller, B., Klemm, E. J., Spooner, E., Claessen, J. H., and Ploegh, H. L. (2008) *Proc. Natl. Acad. Sci. U.S.A.* **105,** 12325–12330
12. Mueller, B., Lilley, B. N., and Ploegh, H. L. (2006) *J. Cell Biol.* **175,** 261–270
13. Lilley, B. N., and Ploegh, H. L. (2005) *Proc. Natl. Acad. Sci. U.S.A.* **102,** 14296–14301
14. Oda, Y., Okada, T., Yoshida, H., Kaufman, R. J., Nagata, K., and Mori, K. (2006) *J. Cell Biol.* **172,** 383–393
15. Younger, J. M., Chen, L., Ren, H. Y., Rosser, M. F., Turnbull, E. L., Fan, C. Y., Patterson, C., and Cyr, D. M. (2006) *Cell* **126,** 571–582
16. Rabu, C., Schmid, V., Schwappach, B., and High, S. (2009) *J. Cell Sci.* **122,** 3605–3612
17. Ernst, R., Mueller, B., Ploegh, H. L., and Schlieker, C. (2009) *Mol. Cell* **36,** 28–38
18. Soneoka, Y., Cannon, P. M., Ramsdale, E. E., Griffiths, J. C., Romano, G., Kingsman, S. M., and Kingsman, A. J. (1995) *Nucleic Acids Res.* **23,** 628–633
19. Oh, R. S., Bai, X., and Rommens, J. M. (2006) *J. Biol. Chem.* **281,** 21480–21490
20. Favaloro, V., Spasic, M., Schwappach, B., and Dobberstein, B. (2008) *J. Cell Sci.* **121,** 1832–1840
21. Ye, Y., Meyer, H. H., and Rapoport, T. A. (2001) *Nature* **414,** 652–656
22. Ye, Y., Meyer, H. H., and Rapoport, T. A. (2003) *J. Cell Biol.* **162,** 71–84
23. Stefanovic, S., and Hegde, R. S. (2007) *Cell* **128,** 1147–1159
24. Mateja, A., Szlachcic, A., Downing, M. E., Dobosz, M., Mariappan, M., Hegde, R. S., and Keenan, R. J. (2009) *Nature* **461,** 361–366
25. Suloway, C. J., Chartron, J. W., Zaslaver, M., and Clemons, W. M., Jr. (2009) *Proc. Natl. Acad. Sci. U.S.A.* **106,** 14849–14854
26. Horn, S. C., Hanna, J., Hirsch, C., Volkwein, C., Schütz, A., Heinemann, U., Sommer, T., and Jarosch, E. (2009) *Mol. Cell* **36,** 782–793
27. Ronchi, P., Colombo, S., Francolini, M., and Borgese, N. (2008) *J. Cell Biol.* **181,** 105–118
28. Nakatsukasa, K., Huyer, G., Michaelis, S., and Brodsky, J. L. (2008) *Cell* **132,** 101–112
29. Schuldiner, M., Metz, J., Schmid, V., Denic, V., Rakwalska, M., Schmitt, H. D., Schwappach, B., and Weissman, J. S. (2008) *Cell* **134,** 634–645